Title

Metabolism and Lung Toxicity of Inhaled Naphthalene: Effects of Postnatal Age and Sex

Journal

Toxicological Sciences, 170(2)

ISSN

1096-6080

Authors

Carratt, Sarah A

Kovalchuk, Nataliia

Ding, Xinxin

et al.

Publication Date

2019-08-01

DOI

10.1093/toxsci/kfz100

Peer reviewed

OXFORD

SOT | Society of Toxicology
www.toxsci.oxfordjournals.org

TOXICOLOGICAL SCIENCES, 170(2), 2019, 536–548

doi: 10.1093/toxsci/kfz100
Advance Access Publication Date: April 24, 2019
Research Article

Metabolism and Lung Toxicity of Inhaled Naphthalene: Effects of Postnatal Age and Sex

Sarah A. Carratt,[*] Nataliia Kovalchuk,[†,‡] Xinxin Ding,[‡,§,1] and Laura S. Van Winkle[*,¶,1]

[*]Center for Health and the Environment, University of California Davis, Davis, California 95616; [†]Wadsworth Center, New York State Department of Health, Albany, New York 12201; [‡]Department of Pharmacology and Toxicology, College of Pharmacy, University of Arizona, Tucson, Arizona 85721; [§]College of Nanoscale Science and Engineering, SUNY Polytechnic Institute, Albany, New York 12203; and [¶]Department of Anatomy, Physiology and Cell Biology, School of Veterinary Medicine, University of California Davis, Davis, California 95616

[1]To whom correspondence should be addressed at Department of Pharmacology and Toxicology, The University of Arizona, College of Pharmacy, 1703 E Mabel Street, Tucson, AZ 85721. Fax: (520) 626-2466; E-mail: xding@pharmacy.arizona.edu and Department of Anatomy, Physiology and Cell Biology, School of Veterinary Medicine, University of California at Davis, One Shields Avenue, Davis, CA 95616. E-mail: lsvanwinkle@ucdavis.edu

ABSTRACT

Human exposure to naphthalene (NA), an acute lung toxicant and possible human carcinogen, is primarily through inhalation. Acute lung toxicity and carcinogenesis are thought to be related because the target sites for both are similar. To understand susceptibility of the developing lung to cytotoxicity of inhaled NA, we exposed neonatal (7 days), juvenile (3 weeks), and adult mice to 5 or 10 ppm NA vapor for 4 h. We measured vacuolated airway epithelium morphometrically, quantified NA and NA-glutathione levels in plasma and lung, and quantified gene expression in microdissected airways. NA inhalation caused airway epithelial cytotoxicity at all ages, in both sexes. Contrary to a previous study that showed the greatest airway epithelial cytotoxicity in neonatal mice following intraperitoneal NA injection, we observed the most extensive airway epithelial toxicity in older, juvenile, animals exposed to NA by inhalation. Juvenile female animals were the most susceptible. Furthermore, NA inhalation in juvenile animals resulted in damage to conducting airway Club cells that was greater in proximal versus distal airways. We also found NA tissue burden and metabolism differed by age. Gene expression pathway analysis was consistent with the premise that female juvenile mice are more predisposed to damage; DNA damage and cancer pathways were upregulated. Our data demonstrate special susceptibility of young, juvenile mice to NA inhalation-induced cytotoxicity, highlight the importance of route of exposure and airway location in toxicity of chemicals in the developing lung, and provide metabolic and molecular insights for further identification of mechanisms underlying age and sex differences in NA toxicity.

Key words: postnatal development; naphthalene; toxicity; gene expression; glutathione.

Naphthalene (NA) is one of the most abundant polycyclic aromatic hydrocarbons in air (Buckpitt *et al.*, 2010; Chuang *et al.*, 1999) and is a respiratory toxicant as well as a possible human carcinogen (USEPA, 1998). The response of the developing lung to NA vapor exposure has not been investigated. This is a concern because children are ubiquitously exposed to NA vapors which are produced by combustion processes. Although there is no information about tumor incidence following childhood NA exposures, there is a correlation between urinary NA metabolites and chromosomal aberrations in T-lymphocytes of children (Orjuela *et al.*, 2012). Elevated NA serum levels have also been linked to asthma in children (Al-Daghri, 2008). Human exposure to NA is widespread (Li *et al.*, 2008), and it is important to consider the effects of continual exposure on susceptible

populations and during critical stages of lung growth and maturation.

A key step in identifying the risk of developmental toxicity is to understand the pattern of acute lung toxicity following NA vapor inhalation in the young. To date, assessment of NA lung toxicity during development has only been investigated in male mice exposed via intraperitoneal (i.p.) injection (Fanucchi *et al.*, 1997a). As an important extension of that study, we have chosen to study both male and female mice, at three developmental stages, following NA *inhalation* exposure. There are advantages and disadvantages to using young mice as a model for human children. Although both species undergo postnatal development of cytochrome P450 (CYP) expression in the lung, the mouse and human CYP isoforms expressed are thought to have inherently different activity levels, which is the basis for a great deal of controversy regarding whether the mode of action for NA is conserved between species (Cruzan *et al.*, 2009). On the other hand, the mouse is a strong model to study Club cell toxicity because Club cells are abundant throughout the airway tree in the mouse, and much is known about the activation/detoxification of NA in the mouse. Further, chronic exposure studies in mice have linked inhalation exposure to NA with formation of lung tumors (Abdo *et al.*, 1992; National Toxicology Program, 1992).

NA requires bioactivation by CYPs monooxygenases to cause airway epithelial cytotoxicity (Buckpitt *et al.*, 1992, 1995; Chichester *et al.*, 1991; Devereux *et al.*, 1989; Li *et al.*, 2011). Inhibition of CYP with piperonyl butoxide results in decreased lung toxicity (Warren *et al.*, 1982); whereas, depleting glutathione (GSH) with diethylmaleate increases toxicity (Warren *et al.*, 1982). A balance of CYP-mediated bioactivation and antioxidant-based detoxification (which can be impacted by GSH abundance and regeneration, and glutathione S-transferase activity/expression) is related to susceptibility [(Phimister *et al.*, 2004; Plopper *et al.*, 2001; West *et al.*, 2000) and reviewed in Buckpitt *et al.* (2002)]. Within the lung, CYPs are focally expressed in specific cell types and locations and their spatial expression can differ during development and maturation. Adult conducting airway nonciliated bronchiolar epithelial Club cells (formerly called Clara cells) (Plopper *et al.*, 1987) are selectively damaged by both inhalation (West *et al.*, 2001) and i.p. administration of NA (Plopper *et al.*, 1992b,c; West *et al.*, 2001) partially due to their high levels of CYPs that are active toward NA (Buckpitt *et al.*, 1995; Chichester *et al.*, 1991; Devereux *et al.*, 1989).

NA is primarily detoxified by phase II enzymes and conjugation to GSH (Fanucchi *et al.*, 2000; Phimister *et al.*, 2004, 2005; Plopper *et al.*, 2001). Studies of injected NA have found that isoform selectivity, abundance and activity of CYPs, and phase II biotransformation enzymes contribute to species (Plopper *et al.*, 1992b,c) and age (Fanucchi *et al.*, 1997a, 2000) differences in airway epithelial toxicity following NA exposure. Airway epithelial CYP expression increases in development, in parallel with the maturation of Club cells. Male National Institutes of Health (NIH) Swiss mice have increasing airway CYP activity with age (Fanucchi *et al.*, 1997b) and mice with immature Club cells are more susceptible than adults to injected NA (Fanucchi *et al.*, 1997a).

Extrapulmonary metabolism of NA is also important. Reactive NA metabolites produced in the liver can be circulated to the lung (Buckpitt and Warren, 1983; Kanekal *et al.*, 1991; Kovalchuk *et al.*, 2017). Human liver microsomes are capable of metabolizing NA to NA-dihydrodiol, 1-naphthol, and 2-naphthol with K_m values in the low micromolar range (Cho *et al.*, 2005). Although humans are thought to be less susceptible to NA than mice because of lower CYP activity in the human lung (in general and toward NA in particular), metabolism in the liver may influence toxicity in the lung through circulation of metabolites.

Inhalation is a major route of environmental exposure to NA. There have been no studies of susceptibility to *inhaled* NA in the developing lung, and the chronic bioassays evaluating NA lung tumor formation were conducted in adult rats (Abdo *et al.*, 2001; National Toxicology Program, 2000) and mice (Abdo *et al.*, 1992; National Toxicology Program, 1992). Earlier studies on the toxicity of i.p. injected NA may not apply to toxicity of inhaled NA, as the toxic outcome of i.p. administered NA may be heavily influenced by metabolites generated in the liver and/or the impact of first-pass metabolism on bioavailability in the target site. The current studies test the hypothesis that NA delivered to developing animals by inhalation will have a different impact on the lung, in terms of site-specific damage and overall susceptibility to toxicity than in the prior study where NA was given intraperitoneally. Because one goal of our study is to probe possible linkages between acute toxicity and the downstream lung cancer outcome of the National Toxicology Program (NTP) studies in mice, we looked beyond the roles of CYP and GSH to understand the impact of NA exposure on a variety of genes involved in disease progression and cell cycle regulation in *both sexes* in the conducting airway injury target region. These experiments define the pattern and location of acute cytotoxicity using quantitative methods and relate this to the dose of NA delivered to the lung and the subsequent conjugation of NA metabolites to GSH. The outcome is placed into the context of the developmental pattern of gene expression, and NA exposure response thereof, by examining key genes involved in bioactivation, detoxification, and carcinogenesis.

MATERIALS AND METHODS

Animals. Adult male and female C57BL/6 mice were purchased from Harlan Labs and were used for breeding. All mice were maintained in a barrier facility with filtered air in AAALAC approved conditions on a 12-h light/dark cycle with food and water *ad libitum*. All animal experiments were performed under protocols approved by the University of California, Davis IACUC in accordance with NIH guidelines.

Whole body inhalation exposure. Male and female C57BL/6 mice (7 days, 3 weeks, 8 weeks) were exposed to NA vapor (5 or 10 ppm) via whole body inhalation for 4 h as described previously (West *et al.*, 2001). Concentration of 10 ppm was selected as the upper limit to correspond with the low dose used in the NTP chronic bioassay and to replicate the Occupational Safety and Health Administration (OSHA) limit for NA exposures in workers. All exposures began between 8 and 9AM PST (2–3 h after the start of the light cycle). Neonatal (7 days) pups were exposed with the dam. Each litter of 7 days pups was normalized to a uniform litter size of 6–9 pups at 1 day to limit differential effects of maternal nutrition in large litters on postnatal growth. Small litters (less than $N = 6$) were excluded from this study. Each litter was considered to be an N of 1, and endpoints were randomized among pups from the same litter so that each endpoint was made up of 5+ litters. Juvenile (3 weeks) pups were exposed postweaning. Animals were euthanized with an overdose of pentobarbital either 24 h after the end of exposure, or within 15 min of the end of exposure. Age-matched control mice were included for comparison. Histopathology was similar for filtered

air exposed mice ($N = 2$, data not shown) and age-matched unexposed controls ($N = 5$–6). Thus, unexposed controls (naive) were used for these studies due to limitations on exposure chamber availability.

High-resolution light microscopy and stereology. Animals ($N = 5$) were sacrificed 24 h after the end of the exposure and exsanguinated. The lungs were removed en bloc and inflated via tracheal cannula at 30 cm of pressure for 1 h with Karnovsky's fixative (0.9% glutaraldehyde/0.7% paraformaldehyde in cacodylate buffer, adjusted to pH 7.4, 330 mOsmol/kg H_2O) as described previously (Van Winkle *et al.*, 2001). Lungs were stored in fixative until use. Karnovsky's fixed tissue samples were embedded separately in Araldite 502 epoxy resin. Specimens were sectioned at 1 μm (Leica Ultracut UCT ultramicrotome with glass knives) and stained with methylene blue/azure II. High magnification images of proximal intrapulmonary airway defined by central location within the lung lobe (to include the mainstem lobar bronchus within three generations as defined by block selection at time of tissue embedment of the left lobe) and terminal bronchioles (defined as having openings to alveolar ducts and limited to the last 200 μm of these airways) were captured using a 20× objective lens using an Olympus BH-2 microscope in bright field mode. Images were converted to grayscale in Adobe Photoshop.

Quantitative measurements of damage were made using the Stereology Toolbox program (Morphometrix, Davis, CA) as previously described (Fanucchi *et al.*, 1997a; Li *et al.*, 2017; Van Winkle *et al.*, 1995). A cycloid test system of known length per point (l/p) was used to perform point (P) and intercept (I) counting on vertical uniform random sections as previously described (Howard and Reed, 1998; Hsia et al., 2010). Volume of damaged epithelial cells per basal lamina surface area (V_s) was calculated to give a quantitative measure of mass of damage ($\mu m^3/\mu m^2$). The formula for this calculation is $V_s = (l/p)(P_d/2I)$, where l/p is the length of cycloid per point at the level of the tissue, P_d is the number of test points hitting structures of interest (damaged epithelial cells), and I is the number of intersections with the epithelial basal lamina. A minimum of 200 points per region of interest (proximal airways, terminal bronchioles) was counted. Damaged epithelial cells were defined as airway epithelial cells attached to the basal lamina that contained cytoplasmic vacuoles. Exfoliated cells that were not attached to the basal lamina were not counted.

NA and NA-GSH in plasma and lung tissue. Animals ($N = 6$–9) were sacrificed within 15 min of the end of the exposure. Blood was collected and placed in Eppendorf tubes on ice, then centrifuged at 20 000 × g for 5 min at 4°C. Supernatant was transferred to new Eppendorf tube and stored at −80°C. Lungs were removed en bloc, rinsed with PBS, and placed in an Eppendorf tube to be stored at −80°C. NA and NA-GSH levels in plasma and lung homogenates were determined using gas chromatography-mass spectrometry and liquid chromatography-mass spectrometry, respectively, as described (Kovalchuk *et al.*, 2017). The limits of detection for NA and NA-GSH were 0.8 and 0.55 pmol, respectively (on column).

NanoString gene expression. For collection of intrapulmonary airway tree samples, the trachea was cannulated and the lungs inflated to capacity with RNAlater (Ambion/Applied Biosystems; Foster City, CA) at 24 h after exposure. The lungs were stored at −20°C until microdissection and RNA isolation could be performed. Conducting airways were microdissected away from parenchymal tissues as previously described (Plopper *et al.*, 1991; Sutherland *et al.*, 2010; Van Winkle *et al.*, 1996). RNA isolation from airways was carried out using the RNeasy Plus Mini Kit (Qiagen; Hilden, Germany) using gDNA eliminator columns. Total RNA concentration and purity was monitored using a NanoDrop spectrophotometer (ThermoFisher; Waltham, MA). Gene expression analysis was performed on 100 ng of RNA per sample using the NanoString nCounter Analysis System (NanoString Technologies; Seattle, WA). The NanoString codeset was custom-designed and composed of 87 genes of interest and 3 housekeeping genes (*Gusb, Actb, Pgk1*). Custom nCounter CodeSet Design Report with probe identifiers and isoform coverage is included in the supplement (Supplementary Table 1). Specific genes of interest included 4 genes to overlap with qRT-PCR and digital PCR methods (*Cyp2F2, Gclm, Ephx1, Scgb1a1*), as well as genes related to GSH synthesis, lung tumors, DNA damage/repair, and xenobiotic metabolism. Raw count data (Supplementary Table 2) was first normalized to the spike-in positive controls to account for assay efficiency, and then normalized to the geometric mean expression value of the five housekeeping genes using nSolver software (NanoString Technologies; Seattle, WA). Data were examined using both nSolver and Ingenuity Pathway Analysis (Qiagen; Hilden, Germany). Causal analysis approaches in Ingenuity Pathway Analysis have been previously described (Kramer *et al.*, 2014).

Statistics and data presentation. GraphPad Prism was used to perform 2-way ANOVA (age, sex) with Tukey's multiple comparisons post hoc test. A 3-way ANOVA (with Tukey's multiple comparisons post hoc test) was run with $n = 5$ per group to examine the effect of sex, age, and airway level on normalized volume of epithelial damage (V_s). Data are reported as mean ± standard error. Values of $p < .05$ were considered statistically significant ($^*p < .05$, $^{**}p < .01$, $^{***}p < .001$, $^{****}p < .0001$). Statistics on figures are shown for significant relationships between males and females of the same age or between different ages within one sex. NanoString gene expression data were analyzed using nSolver software (NanoString Technologies; Seattle, WA; www.nanostring.com) and Ingenuity Pathway Analysis (Qiagen; Hilden, Germany). nSolver utilized R3.1.1 (R Foundation for Statistical Computing; Vienna, Austria; www.r-project.org) and XQuartz (www.xquartz.org) to run software for Mac. Significance for NanoString data were determined using $p < .05$ with false discovery rate of 25%. Fold change on figures is displayed for measurements greater than 1.2 or less than −1.2, with a p value cutoff of .05. Multipanel figures were prepared in Adobe Illustrator CC 2017 (Adobe Systems; San Jose, CA; http://www.adobe.com/products/illustrator.html).

RESULTS

Qualitative Histology

Inhalation of NA caused airway epithelial cytotoxicity at all airway levels examined, in all ages and in both sexes. Airway epithelial cytotoxicity was evident both as Club cell swelling and by the formation of cytoplasmic vacuoles within damaged Club cells (Figure 1). This toxicity was specific for airway epithelial Club cells, and other cell types within the airway and alveolar epithelium were not affected. In female juvenile and adult mice, the swollen Club cells were more abundant in proximal airways than in distal airways, distributed in clusters. Of all airway levels and groups, the proximal airways of juvenile female mice contained the greatest abundance of swollen and

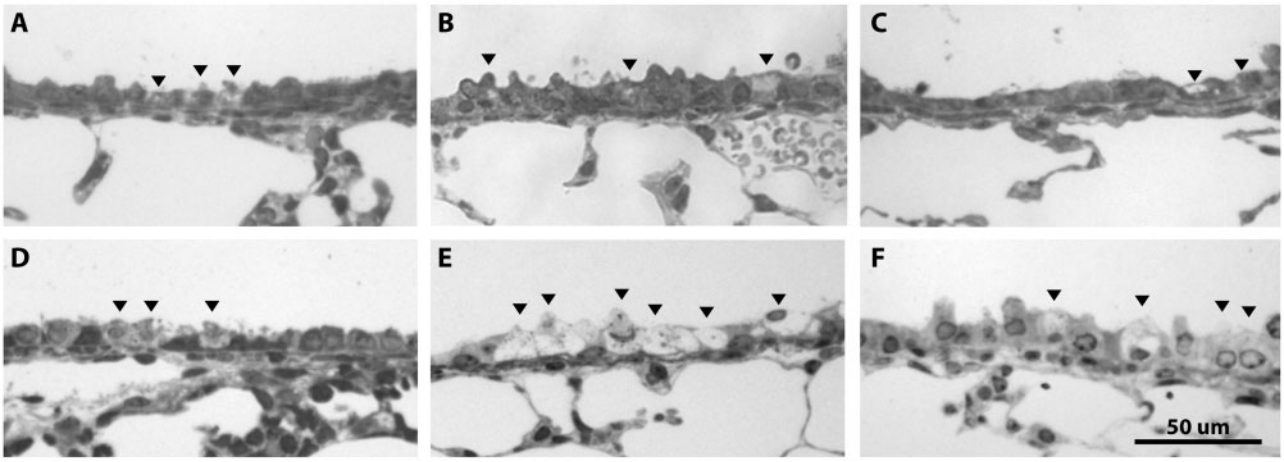

Figure 1. Proximal airway epithelial damage (swelling and vacuolization) was evident at all ages following 10-ppm NA exposure, but was most severe for the juvenile female group. A, Neonatal male, B, juvenile male, C, adult male, D, neonatal female, E, juvenile female, and F, adult female. These representative images show sex and age differences in cellular vacuolization and swelling for the proximal airways following 10-ppm NA exposure ($n = 5$). Black arrowheads show damaged Club cells.

vacuolated Club cells, and the degree of swelling was the most severe. The change in Club cell morphology, which corresponded with increasing concentrations of NA, is shown in Figure 2 for juvenile female proximal airways and terminal bronchioles. Vacuolated cells were present in all airway levels beginning at 5 ppm, with increased vacuolization in the proximal airways at 10 ppm.

Quantitative Stereology

Quantification of epithelial damage through stereology point-intercept counting supported our qualitative observations that the juvenile female proximal airway was most severely damaged by NA inhalation, and that damage from inhalation was primarily to proximal conducting airways within each lung lobe. Epithelial damage is expressed as V_s, mass of epithelium containing vacuolated cells per length of basal lamina ($\mu m^3/\mu m^2$) in Figure 3. All exposed tissues had a significantly higher mass of vacuolated conducting airway epithelium than controls. Mass of vacuolated epithelium in the controls ranged from 0.00 to 0.13 $\mu m^3/\mu m^2$. The effects of age and sex on mass of vacuolated proximal airway epithelium (V_s) were examined using a 2-way ANOVA (Figure 3A). There was not an interaction between sex and age $F(2, 24) = 1.6$, $p = .21$, though the main effect of age was significant ($F(2, 24) = 3.5$, $p = .047$). The mass of vacuolated epithelium in the proximal airway of juvenile female ($3.2 \pm 1.2\ \mu m^3/\mu m^2$) was approximately 4.6-fold greater than in the neonatal female ($0.69 \pm 0.25\ \mu m^3/\mu m^2$, $p = .017$). The mass of vacuolated terminal bronchiole airway epithelium (Figure 3B) was not affected by age ($F(2, 24) = 0.49$, $p = .62$) or sex ($F(1, 24) = 0.27$, $p = .61$), or by a combination of these 2 factors ($F(2, 24) = 0.61$, $p = .55$).

Lung and Plasma NA

When measured at the end of a 4-h whole body inhalation exposure, the highest level of unmetabolized NA in lung tissue (Figure 4A) was in the male adult (11 ± 2.9 ng NA/g lung tissue), which was approximately 1.8- to 5.5-fold higher than other ages and sexes (Figure 4). Among other groups, the levels of parent NA in lung tissue were statistically similar (Figure 4A). However, age and sex both independently affected levels of NA in lung tissue, with no interaction between age and sex ($F(2, 30) = 1.3$, $p = .29$). Age accounted for approximately 26% of the variance ($F(2, 30) = 6.6$, $p = .0041$) and sex accounted for approximately 9.1% of the variance ($F(1, 30) = 4.6$, $p = .040$).

NA concentration in plasma (Figure 4C) was highest in adult and juvenile mice (10–15 pg NA/μL plasma) and lowest in neonatal mice (4.6–5.4 pg NA/μL plasma). Juveniles had 2.2-fold (male, $p = .0020$) to 2.8-fold (female, $p < .0001$) higher levels of NA in plasma than neonates. The only significant sex difference between animals of the same age was between juvenile females and juvenile males, where juvenile females have 1.5-fold higher NA concentration in plasma (Figure 4C, $p = .0065$). Age was the primary driver of differences in plasma NA levels, accounting for about 64% of the variation ($F(2, 35) = 52$, $p < .0001$); however the effect of sex was also significant and accounts for 8% of the variation ($F(1, 35) = 13$, $p = .0010$). There was no interaction between sex and age ($F(2, 35) = 15$, $p = .086$).

Lung and Plasma NA-GSH

Neonatal females had 1.8-fold higher levels of NA-GSH in lung tissue than juvenile females ($p = .042$), while all other groups were statistically similar (Figure 4B). Neonatal male mice had an average of 64 ± 13 ng NA-GSH/g lung tissue, while juveniles and adults had 43–46 ng NA-GSH/g lung tissue. Neonatal female mice had an average of 79 ± 10 ng NA-GSH/g lung tissue, while juveniles and adults had 44–58 ng NA-GSH/g lung tissue (Figure 4B). Approximately, 26% of the variance in the levels of NA-GSH in lung can be explained by age alone ($F(2, 31) = 6.1$, $p = .0060$), while sex had no effect ($F(1, 31) = 2.0$, $p = .17$). There was no interaction between the main effects of age and sex ($F(2, 31) = 0.80$, $p = .46$).

Plasma levels of NA-GSH were low (relative to adults) for both male (26 ± 2.0 pg NA-GSH/μL plasma) and female (27 ± 3.2 pg NA-GSH/μL plasma) neonatal mice (Figure 4D). Plasma NA-GSH levels increased significantly with age, and age independently accounted for 60% of the total variance ($F(2, 37) = 32$, $p < .0001$). Adult male mice had 1.5-fold higher plasma NA-GSH than juveniles ($p = .011$), and 2.0-fold higher than neonates ($p < .0001$). Adult female mice did not have significantly higher levels of NA-GSH than juveniles ($p = .81$), but both juveniles ($p = .0017$) and adults ($p = .0002$) had higher levels than neonates (Figure 4D).

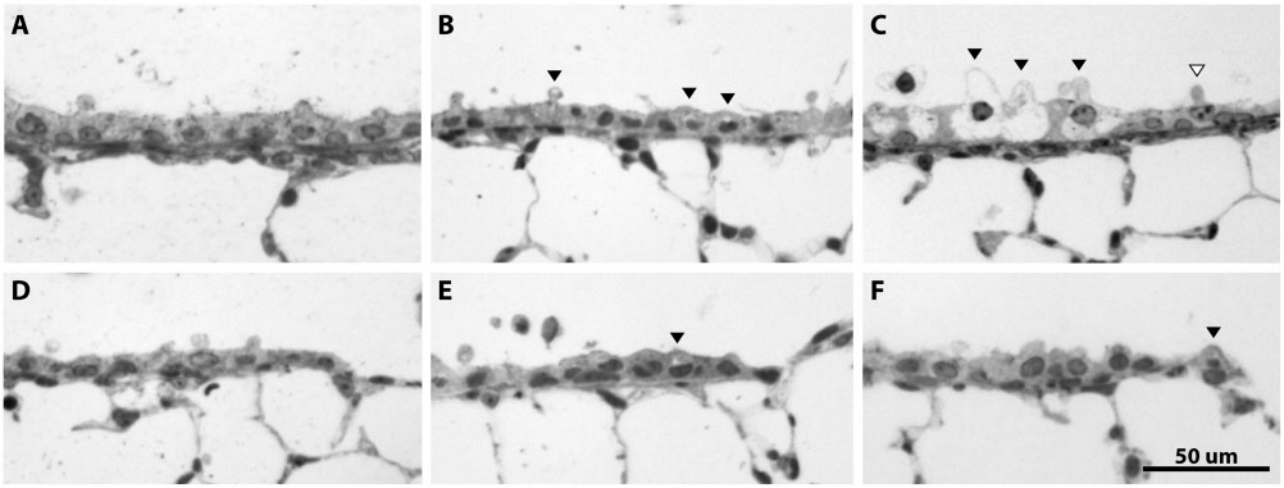

Figure 2. The extent and severity of NA damage was greater in the proximal airways than in the terminal bronchioles (distal airways). A, Naive proximal airway, B, proximal airway at 5 ppm, C, proximal airway at 10 ppm, D, naive terminal bronchiole, E, terminal bronchiole at 5 ppm, and F, terminal bronchiole at 10 ppm. These representative images show the pattern of dose-dependent cellular damage following NA inhalation for juvenile female mice. Cytoplasmic vacuoles were present in all airway levels beginning at 5 ppm, with increased vacuolization in the proximal airways at 10 ppm. Many Club cells in the juvenile female proximal airways were swollen. Black arrowheads show damaged Club cells; white arrowhead shows undamaged Club cell for size reference at 10 ppm.

Conducting Airway Specific Gene Expression

We used microdissected tissue to isolate the injury target region, the conducting airways, and specifically measured gene expression at this site. Gene expression specifically in the conducting airways of naive, unexposed mice is presented as a ratio relative to adults of the same sex (Table 1 and Figure 5). Table 1 lists the CYP- and GSH- related genes that were changed in neonate and juvenile animals compared with adults of each respective sex. There are substantial changes in gene expression with age in both sexes underscoring the postnatal development of these genes. In Figure 5, the degree of gene enrichment (fold over adult of same sex) was greater for neonates than for juveniles for all 10 disease and disorder functions of interest (Figure 5A: cancer; cell cycle; cell death and survival; cell morphology; cellular development; cellular function and maintenance; cellular growth and proliferation; DNA replication, recombination, repair; respiratory disease, tumor morphology). The ranking order for gene enrichment (fold over adult of same sex) across all groups followed the pattern: male neonate > female neonate > male juvenile > female juvenile. Fold changes (increase = red, decrease = green) are displayed for genes associated with *lung tumors* (Figure 5B), *DNA damage* (Figure 5C), and *repair of DNA* (Figure 5D) pathways. These data are also presented graphically in Figures 5E and 5F (cutoff $p = .05$, |fold-change|≥1.2). The categories for gene enrichment (Figure 5A) and pathway analysis (Figs. 5B–F) are defined by the Ingenuity Pathway Analysis (IPA) software, based on biological interactions and functional annotations from primary literature, and public and third-party databases. Gene enrichment analysis allows the identification of gene networks (ie, cancer, cellular development) that were differentially expressed with age or NA exposure.

All significant age-related gene expression changes with an effect size greater than or equal to 1.2-fold are reported in Supplementary Table 3 for samples from naive (control) animals. With a fold-change cutoff of 1.2, the number of genes with modified expression level from adult for each age group was: 68 (neonate male), 24 (juvenile male), 66 (neonate female), and 17 (juvenile female). Many of these genes were related to antioxidant and glutathione processes, and their expression was lower in younger animals (Table 1). This is consistent with previous observations of Phase II and Cyp expression during rodent lung development (Chan *et al.*, 2013; Fanucchi *et al.*, 2000, 1997b). Genes that were low in neonates relative to adults (5-fold or greater) include: *Cyp2f2, Gsta3, Gpx6, Gpx3, Spp1, Cyp19a1*, and *Dsg3* (*Cdkn2a*, *Scgb1a1* 5× in females only; *Ptgs2* 5× in males only). The greatest fold change relative to adult was seen for *Inmt*, which was markedly lower in neonates (57.2-fold in males, 70.0-fold in females). Although little-to-no information is available about the role of these genes in lung development, the elevated *Inmt* expression observed in this study is consistent with a study in rabbits that showed *Inmt* protein expression and enzyme activity increases after birth (Lin *et al.*, 1974).

Genes that were expressed at higher levels in neonates or juveniles than in adults include *Actb* (housekeeping), *Ahr*, ***Birc5***, *Cdkn1c, Gpx7, Gstm5*, ***Mki67***, *Pcna*, ***Thbs2***, ***Top2a***, *Trp53*, ***Wifi1*** (**bold**: 2-fold or higher in both sexes). Notably, age-related changes in gene expression were not always linear. There are a number of genes for which expression in the juvenile airway was higher than in the neonate and adult. For juvenile females—who may be predisposed to NA toxicity based on the morphological data—these genes included *Agr2, Cdkn1c, Ephx2, Fabp4, Gadd45g, Gsta3, Gstm3, Gstm5, Mgst3, Pgk1, Ptgs2*. For juvenile males, these genes included *Agr2, Egfr, Pgk1*.

Gene expression data are presented in Table 2 and Figure 6 as a ratio of exposed (10 ppm NA) to unexposed. For *cancer* and *tumor morphology*, gene enrichment (fold over unexposed) followed the pattern: juvenile male > adult female > neonate male > adult male > juvenile female > neonate female (Figure 6A). There is currently no data about lung tumor development in young animals following NA exposure; however, it has been established that lung tumors form following chronic NA inhalation in the lungs of female mice, but not males (Abdo *et al.*, 1992; National Toxicology Program, 1992). In our dataset, *lung tumors* (an IPA identified gene pathway) were predicted to be "activated" in adult airways, in both sexes (Figs. 6E and 6F). *DNA damage* (IPA identified pathway) was slightly increased with NA exposure in females, but slightly decreased in males. *DNA repair* (IPA identified pathway) was strongly increased with NA in males, but weakly decreased in females (Figs. 6E and 6F). The

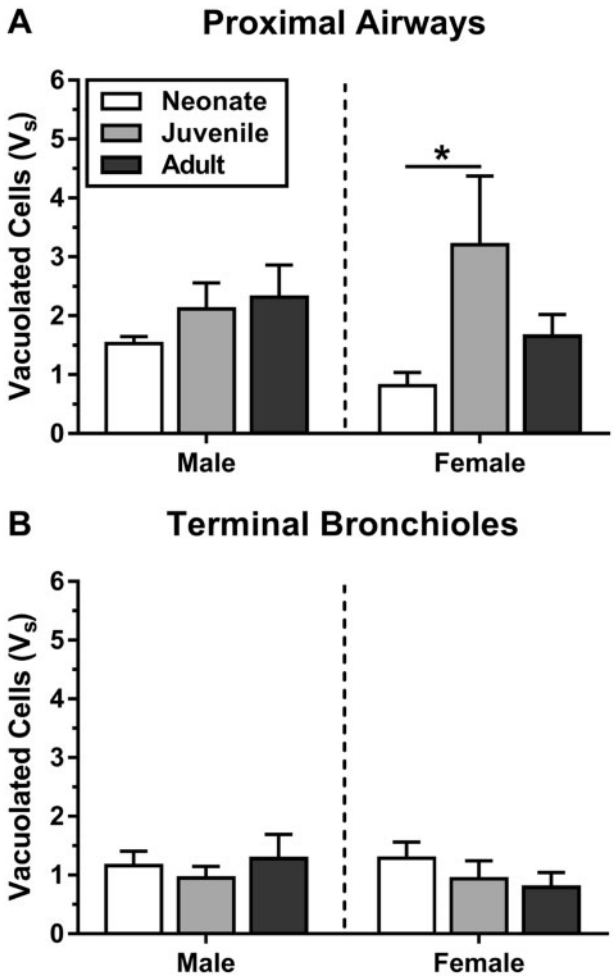

Figure 3. At 10 ppm, juvenile females had high levels of vacuolated epithelium in the proximal airways, as measured by morphometric approaches. Epithelial damage (V_s) is defined as volume of epithelium containing vacuolated cells, normalized to basal lamina surface area ($\mu m^3/\mu m^2$). Mass of vacuolated epithelium in the controls ranged from 0.00 to 0.13 $\mu m^3/\mu m^2$. These measurements confirmed that proximal airways (A) have a greater volume of epithelial damage per basal lamina than distal airways (terminal bronchioles) (B) at 10 ppm. Statistics ($n = 5$): 2-way ANOVA (age, sex) with Tukey's post hoc test (*$p < .05$).

individual genes driving these pathway differences were as follows. *Birc5* (1.58-fold, $p = .017$) and *Top2a* (1.87-fold, $p = .004$) was increased with exposure in (Figure 6F) adult females, but not (Figure 6E) adult males. *Ptges* (1.34-fold, $p = .046$), *Agr2* (2.99-fold, $p = .027$) was decreased with exposure in adult females only. *Gclc* (1.58-fold, $p = .024$) was increased with exposure in male adults only. *Krt14* (1.81-fold, $p = .024$), *Nqo1* (1.30-fold, $p = .0009$), and *Thbs2* (1.47-fold, $p = .023$) were decreased with exposure in male adults only.

Following NA exposure, we observed significant gene expression changes in the juvenile female that are not observed in males or females of other ages or in males. *Col11a1* (2.6-fold, $p = .033$) and *Lig4* (1.33-fold, $p = .02$) were significantly downregulated in only the juvenile female. *Sprr1a* (small proline rich protein 1A) was highly upregulated with exposure in the juvenile female (30.6-fold, $p < .0001$), and to a lesser degree in the adult male (8.75-fold, $p = .003$) and female (6.37-fold, $p < .0001$). The only gene significantly increased with exposure in juveniles and adults of both sexes was *Cxcl13* (3.14- to 3.96-fold).

A number of genes are expressed at lower levels in exposed airways than naive airways. In juvenile and adult groups, these genes included *Cyp2f2* (4.79- to 9.54-fold), *Scgb1a1* (2.27- to 4.26-fold), and many glutathione synthesis and metabolism genes (*Gpx6*, *Gsta3*, *Mgst1*, *Eef1b2*, *Gsta4*, *Mgst2*, *Gstk1*, *Hnmt*, *Gstm4*). All significant exposure-induced gene expression changes with an effect size greater than or equal to 1.2-fold are reported in Supplementary Table 4 and the CYP and GSH-related gene subsets are also listed in Table 2. Enlarged versions of Figures 5E and F and 6E and F are included as Supplementary Figures 1–4.

DISCUSSION

Our data highlight the importance of route of exposure and airway location in toxicity of chemicals in the developing lung. Contrary to previous studies of i.p. injected NA that found the youngest animals (7 days) to be the most susceptible (Fanucchi *et al.*, 1997a), we found that older juvenile (3 weeks) animals exposed to NA vapor were more sensitive than neonates, with the female juveniles being the most susceptible. Furthermore, NA inhalation in juvenile animals resulted in damage to conducting airway Club cells that was greater in proximal than in distal airways (Figure 3). The opposite has been shown in neonatal and adult animals (distal > proximal) following i.p. NA injection (Fanucchi *et al.*, 1997a; West *et al.*, 2001). We also found that NA tissue burden and metabolism differed by age, but not as much by sex (Figure 4). Baseline developmental patterns of conducting airway gene expression in naive mice are consistent with the notion that female juvenile mice are more predisposed to *DNA damage* and *lung tumors* than adult or neonatal mice of either sex.

Following NA inhalation, epithelial damage was observed in both proximal and distal airways of all mice studied (Figure 3). The extent of injury in the proximal airway epithelium was either similar to (7 days) or more severe (3 weeks and adult) than in the terminal bronchiolar epithelium. This contrasts with data from the only other NA postnatal development study, which used i.p. NA injection; that study found relatively little damage in the proximal airways of 7 or 14 days male mice, but severe damage in the terminal bronchiolar epithelium (Fanucchi *et al.*, 1997a). Injury in the larger (proximal) airways observed in the present study for adult mice is consistent with the inhalation route of exposure and known injury target sites in adult male mice by either NA inhalation or i.p. injection (West *et al.*, 2001). We have confirmed that Club cells are the target of NA toxicity regardless of route of exposure (or sex) in the postnatal period. However, the target *region* within the conducting airway tree varies by route of exposure, likely reflecting local concentration of the toxicant. Taken together, this underscores the concept that the route of exposure can heavily influence the location of cytotoxicity.

Age differences in sensitivity to NA-induced airway epithelial toxicity corresponded with the gene expression data showing decreases in two Club cell markers, *Cyp2f2* (highly expressed in Club cells) and *Scgb1a1* (Club cell secretory protein), in exposed juvenile and adult airways relative to naive airways. The greatest exposure-related decrease in *Cyp2f2* and *Scgb1a1 expression* was in juvenile females (Supplementary Table 4), a finding consistent with the greatest loss of Club cells in this group. Thus, the histopathology data and the gene expression data both support the conclusion that female mice are at least as susceptible as males to NA vapor-induced airway toxicity, and that juvenile female mice are the most susceptible, at or below the current OSHA standard for human exposure to NA, 10 ppm. It should be noted, however, that it is difficult to directly relate these findings to susceptibility in humans, because rodents,

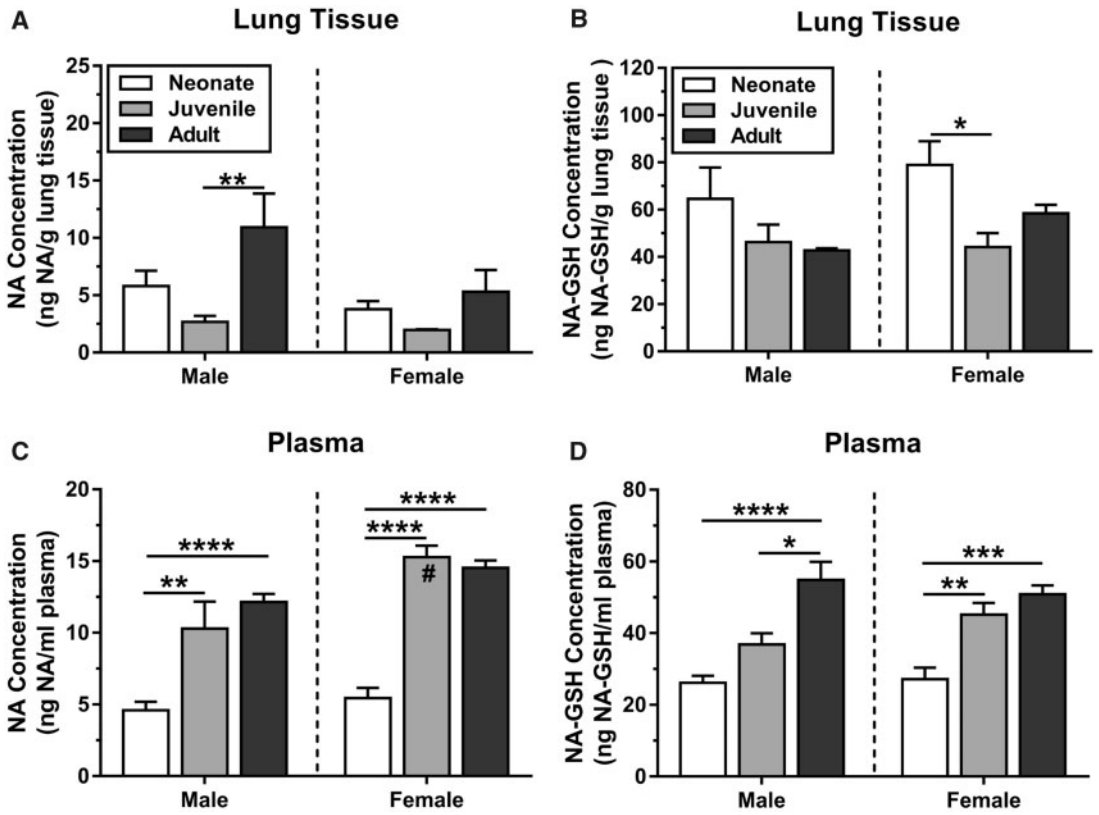

Figure 4. Levels of (A, C) unmetabolized and (B, D) GSH-conjugated NA in plasma and lung tissue. Levels of unmetabolized NA were low in juvenile lung tissue (ng/g) and high in juvenile plasma (ng/ml). Neonatal mice had high levels of NA-GSH (ng/g) in lung tissue, but this group had the lowest levels of NA-GSH in plasma (ng/ml). Tissue collected 0–15 min after 10 ppm × 4 h exposure. NA concentration in juvenile female plasma was significantly higher than in juvenile males and female neonatal mice. Statistics ($n = 6$–8): 2-way ANOVA (age, sex) with Tukey's post hoc test (*$p < .05$, **$p < .01$, ***$p < .001$, ****$p < .0001$; #, significantly greater than juvenile male, $p = .0065$).

due to their obligate nose breathing and the first-pass clearance by the nasal mucosa, likely have a lower delivered dose to the lung than in humans. Further, there are cell biology and metabolism differences between mice and humans that could affect susceptibility, some of which could be studied using human lung cells incubated with NA *in vitro*.

In addition to Club cell cytotoxicity, we identified a number of toxicity-related genes with significant expression changes following NA exposure. Among these, a few are of particular note for their pattern of expression in the juvenile female mice. *Sprr1a* (small proline rich protein 1A) is highly upregulated by NA exposure in the juvenile female (30.6-fold). Amplified *Sprr1a* expression in cultured airway epithelium is known to be associated with squamous metaplasia (An *et al.*, 1993; Tesfaigzi *et al.*, 1996) and lung squamous cell carcinoma (Hawthorn *et al.*, 2006). *Col11a1* (collagen, type XI, alpha 1) and *Lig4* (ligase IV, DNA, ATP-dependent) were significantly *downregulated* in only the juvenile female. The implication of this latter finding is unclear, but the decrease in *Col11a1* may lead to a deficit in wound repair following acute NA injury. On the other hand, increases in *Col11a1* expression is known to be associated with nonsmall cell lung cancer (Navab *et al.*, 2011; Shen *et al.*, 2016) and adenocarcinoma (Wang *et al.*, 2002). In fact, *Col11a1* is used as a diagnostic marker for nonsmall cell lung cancer in human patients (Shen *et al.*, 2016). For *Lig4*, which is involved in double-strand DNA break repair through nonhomologous end-joining (Sengupta and Harris, 2005), a decreased expression may lead to greater probability of mutagenesis. Recently, it has been shown that both NA and its 1,2-napthoquinone metabolite are capable of adducting DNA in adult male and female mouse and primate lung tissue (Buchholz *et al.*, 2019; Carratt *et al.*, 2019). Further studies to follow the outcome of an inhalation exposure in juvenile females over time would be needed to understand the effect of this expression pattern on long-term lung health.

Within the mouse terminal bronchiolar airways, the abundance of Club cells shifts slightly during postnatal development; Club cells in the terminal bronchiole, the most distal conducting airways, increase in numbers by approximately 1.5-fold between 7 days of age and adulthood, when Club cells comprise >75% of the terminal bronchiolar epithelium (Plopper and Hyde, 1992a). However, although the number changes are not large in terms of percent of the epithelial population, there is a substantial postnatal maturation of enzyme systems within Club cells. Furthermore, it is important to underscore that, although enriched in Club cells, the microdissected conducting airways function as an epithelial-mesenchymal trophic unit (Evans *et al.*, 1999), and contain other cell types including smooth muscle cells, fibroblasts, and ciliated cells, all of which contribute to the overall expression pattern measured in the dissected airways. So, while the airway microdissection method significantly enriches for airway epithelial cells in the RNA sample (especially compared with whole lung isolates), it is not specific to a single cell type. Also, because we dissected the whole airway tree and did not subdivide it by target regions, the toxic responses may be further diluted. Future studies could use the injury site information we have developed here for each age to conduct a more targeted analysis.

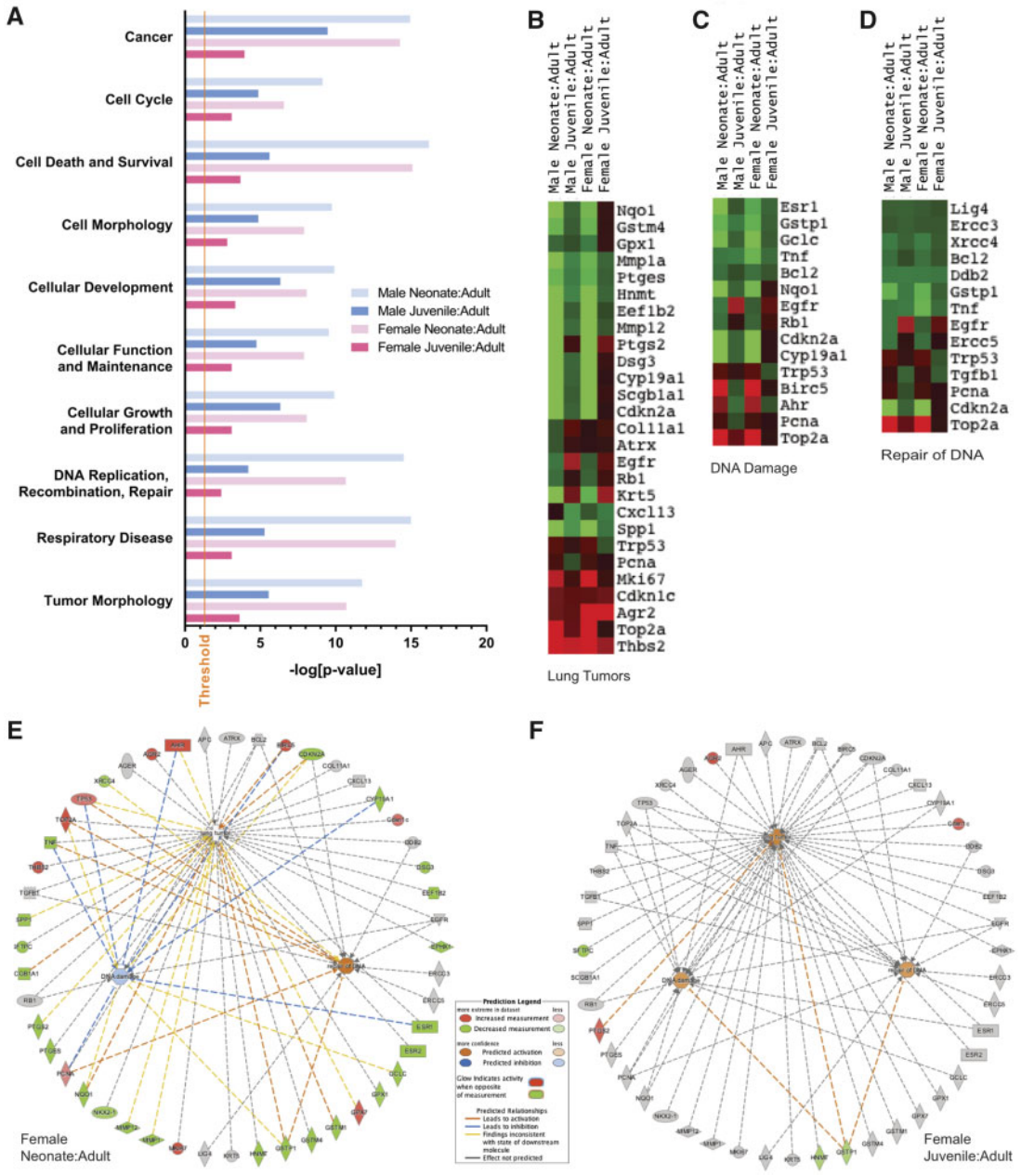

Figure 5. Gene expression in unexposed young mice relative to adults of the same sex. A, Gene enrichment for selected relevant disease and disorder functions with significance as determined by IPA software using Fisher's exact test. Threshold for significance is set at –log (0.05). B–D, Heatmaps for groups of genes associated with B, lung tumors, C, DNA damage, or D, repair of DNA. E–F, Genes associated with lung tumors or DNA damage/repair with IPA prediction of activation (orange) and inhibition (blue), and with observed increases (red) or decreases (green) in young female animals relative to female adults. Gene expression is lower in neonates than adults for most genes of interest. Gene expression is similar between juveniles and adults for most genes of interest; however three genes (*Agr2*, *Cdkn1c*, *Ptgs2*) have increased measurement and three (*Sftpc*, *Hnmt*, *Gstp1*) have decreased measurement.

Pathway analysis, based on expression changes in all genes examined, indicates that, for both males (Figure 6E) and females (Figure 6F), *lung tumor pathways* were "activated" by NA exposure. *DNA damage* was slightly increased with NA exposure in females, but slightly decreased in males. *DNA repair* was strongly increased with NA in males, but weakly decreased in females (Figure 6). Notably, NA exposure causes the death and exfoliation of Club cells; therefore, the overall differences in airway gene expression were modified by enrichment of non-Club cell "survivor" populations, which may have different baseline expressions than Club cells. Regardless, these data reveal not only the potential for NA to induce lung carcinogenesis, but also sex differences in multiple genes that are up- or downregulated by NA exposure. The significance of the sexually dimorphic gene expression responses to NA exposure for the reported female selectivity of lung carcinogenesis following chronic NA exposure remains to be determined as animals in these younger aged exposure groups have not had long-term follow-up studies.

NA toxicity is dependent on bioactivation (Buckpitt *et al.*, 1992, 1995; Chichester *et al.*, 1991; Devereux *et al.*, 1989; Li *et al.*, 2011), with the initial step being CYP-mediated NA

Table 1. Significantly Changed CYP- and GSH-Related Genes in Neonate and Juvenile Versus Adult Airways

		Fold Change Relative to Adult of Respective Sex			
Gene	Gene Name	Female Neonate	Female Juvenile	Male Neonate	Male Juvenile
Cyp19a1	Cytochrome P450, family 19, subfamily a, polypeptide 1	−5.39		−5.01	
Cyp2f2	Cytochrome P450, family 2, subfamily f, polypeptide 2	−8.11		−8.01	
Gclc	Glutamate-cysteine ligase, catalytic subunit	−2.85		−2.77	
Gclm	Glutamate-cysteine ligase, modifier subunit	−1.48		−1.52	
Gpx1	Glutathione peroxidase 1	−1.52		−1.27	
Gpx3	Glutathione peroxidase 3	−9.41		−6.47	
Gpx4	Glutathione peroxidase 4	−2.37	−1.29	−2.00	
Gpx5	Glutathione peroxidase 5	−2.70		−1.51	
Gpx6	Glutathione peroxidase 6	−9.70		−6.69	
Gpx7	Glutathione peroxidase 7	1.77		1.93	1.46
Gsr	Glutathione reductase	−1.62		−1.91	−1.39
Gss	Glutathione synthetase	−1.90		−1.87	
Gsta3	Glutathione S-transferase, alpha 3	−7.57	1.56	−7.75	
Gsta4	Glutathione S-transferase, alpha 4	−2.83		−3.36	
Gstk1	Glutathione S-transferase kappa 1	−2.06		−1.87	
Gstm2	Glutathione S-transferase, mu 2	−3.08		−2.59	
Gstm3	Glutathione S-transferase, mu 3	−2.06	1.57	−4.17	−1.86
Gstm4	Glutathione S-transferase, mu 4	−2.35		−2.40	
Gstm5	Glutathione S-transferase, mu 5	1.26	1.31	1.20	
Gsto2	Glutathione S-transferase omega 2	−2.00		−1.57	
Gstp1	Glutathione S-transferase, pi 1	−2.24	−1.22	−2.29	−1.49
Gstt1	Glutathione S-transferase, theta 1	−1.95	−1.70	−1.62	−2.13
Gstt2	Glutathione S-transferase, theta 2	−1.74		−1.70	

epoxygenation, which can occur in both the lung and the liver (Buckpitt and Warren, 1983; Buckpitt *et al.*, 1992). Thus, the age- and sex-specific differences in NA lung toxicity may be due to differences in rates of NA bioactivation. The primary reactive metabolite of NA, NA oxide, readily forms glutathione conjugates, which can be used as an indirect measure of the amounts of NA oxide produced *in vivo*. Interestingly, age-related differences were found in NA and NA-GSH levels in plasma and lung tissue of NA-exposed mice, although a sex difference was not observed. The reason for the age-related difference in NA and NA-GSH levels remains to be identified, but it may involve age-dependent changes in both NA delivery and disposition. Importantly, the NA and NA-GSH data do not explain the unique susceptibility of the juvenile *female* to NA toxicity, given that neither plasma nor lung levels of NA or NA-GSH were uniquely elevated in this group, compared with other groups. Nonetheless, our data do not exclude the possibility that further metabolites of NA oxide, such as NA quinones, which are also believed to be cytotoxic (Chichester *et al.*, 1994), are preferentially produced in the juvenile female, and are thus responsible for the age- and sex-specific enhancement in NA toxicity. Further studies of *in vivo* formation of downstream NA metabolites are warrantied.

The formation of NA-GSH is a detoxification mechanism for NA. The ability of the lung to continue to conjugate NA oxide to GSH, thereby removing NA oxide from the lung, is influenced by the availability of GSH in the lung tissue and indirectly by the activity of GSH-synthesizing enzymes in surviving airway epithelial cells. Consequently, the hypersensitivity of juvenile female mice to NA toxicity might also be due to an age- and sex-specific deficit in the ability to synthesize GSH in the lung. In adult, male NIH Swiss mice, GSH depletion is an early event that affects all airway generations, with maximal GSH depletion occurring at 2–4 h after the start of a 15-ppm inhalation exposure (Phimister *et al.*, 2004). Synthesis of new GSH following adult *ex vivo* NA exposure occurs over 6 h, with high efficiency in the parenchyma and the minor daughter airways (Duan *et al.*, 1996). It has been suggested that low levels of NA may be sufficient to deplete GSH in target cell populations of neonatal animals (Fanucchi *et al.*, 2000) and that cells are unable to upregulate GSH synthesis sufficiently in response at very young ages (Chan *et al.*, 2013). However, the neonatal pups in our study had the highest levels of NA-GSH in lung tissue and the least severe cytotoxicity. This suggests that the neonatal mouse lung has sufficiently large GSH reservoirs to protect against NA inhalation exposure; but it remains to be determined whether GSH synthesis is limiting in NA-exposed juvenile female mice.

The differing sensitivities of the neonatal lung to i.p. and inhaled NA are also intriguing. It is possible that the relatively high susceptibility of the neonatal lung, compared with adult lung, to NA toxicity in the previous i.p. study (Fanucchi *et al.*, 1997a) was driven by the formation of greater amounts of reactive NA metabolites in the liver during first-pass metabolism, or by insufficient liver detoxification of NA oxide via GSH conjugation in the neonates. It has been suggested previously that reactive NA metabolites that are produced *in vivo* in the liver can circulate to the lung (Buckpitt and Warren, 1983; Kanekal *et al.*, 1991), and hepatic CYP contribution to lung toxicity induced by inhaled NA has been demonstrated recently (Kovalchuk *et al.*, 2017). However, the hepatic contribution to lung toxicity would be less prominent with inhalation NA exposure than with i.p. NA administration, given the lower amounts of NA reaching the liver following inhalation than following i.p. injection. Future studies could examine this in more detail by determining the levels of various NA metabolites in the two different NA exposure routes.

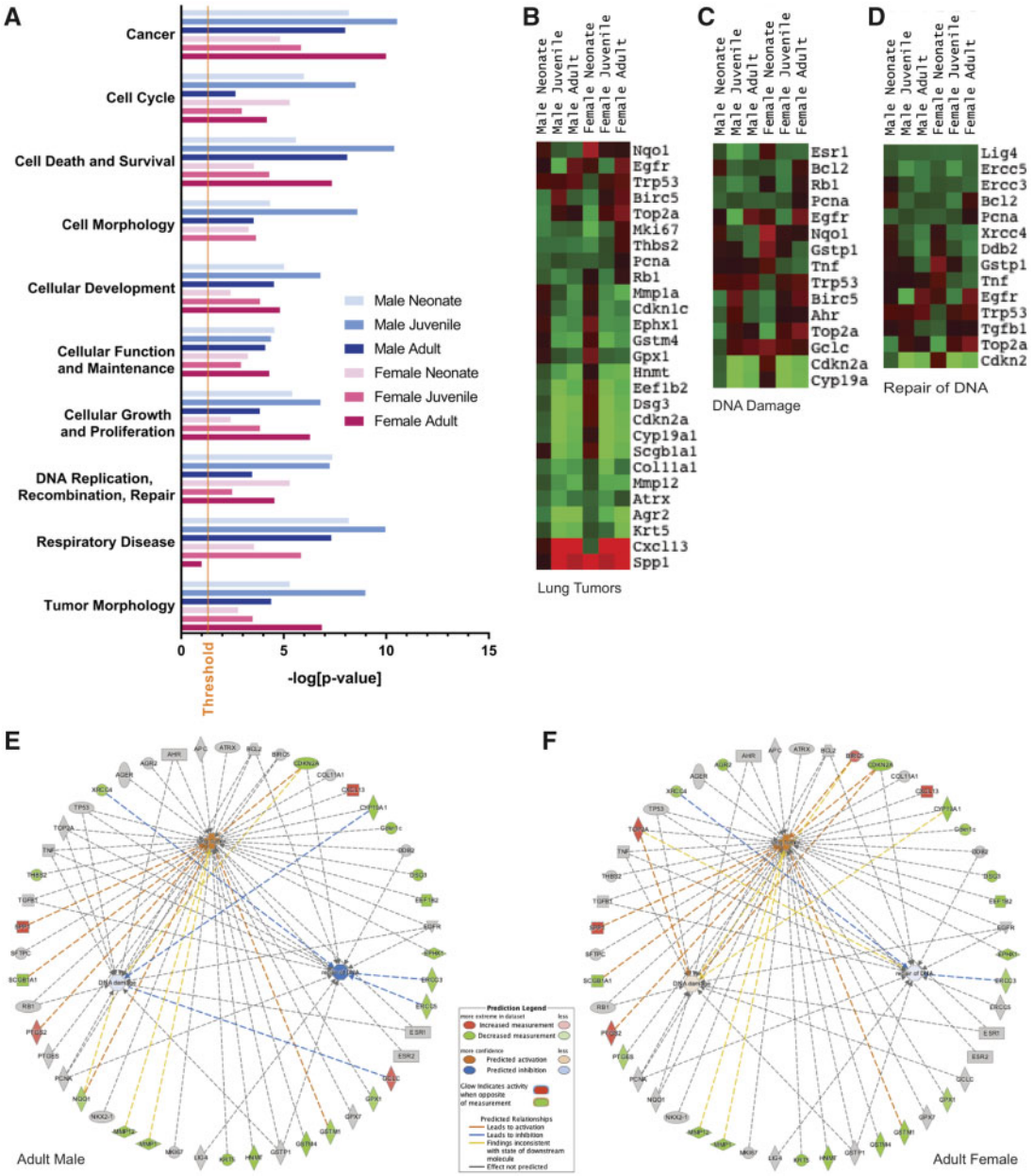

Figure 6. Gene expression in 10-ppm NA-exposed mice relative to unexposed, age-matched animals. A, Gene enrichment for selected relevant disease and disorder functions with significance as determined by IPA software using Fisher's exact test. Threshold for significance is set at –log (0.05). B–D, Heatmaps for groups of genes associated with B, lung tumors, C, DNA damage, or D, repair of DNA. E–F, Genes associated with lung tumors or DNA damage/repair with IPA prediction of activation (orange) and inhibition (blue), and with observed increases (red) or decreases (green). Lung tumors are predicted to be inhibited in both sexes, with predicted activation of DNA damage pathways in females only. *Birc5* and *Top2a* are activated with exposure in (F) adult females, but not (E) adult males. *Ptges, Agr2* is decreased with exposure in adult females only. *Gclc* is activated with exposure in male adults only. *Krt14, Nqo1, Thbs2* are decreased with exposure in male adults only.

Conclusions

The proximal airways of juvenile female C57BL/6 mice were uniquely hypersensitive to inhaled NA; cytotoxicity in the juvenile female proximal airways was between 1.4- and 4.6-fold greater than other exposed groups. The mechanism underlying this age and sex difference in susceptibility is unclear, but it appears to be unrelated to variations in the primary NA bioactivation step in the lung or the conjugation of GSH with NA oxide, though the NA tissue burden and metabolism differed by age. NA inhalation exposure induces the expression of several genes or pathways related to lung tumor development, but with minor differences between males and females. Gene expression data in naive mice were consistent with the concept that female juvenile mice are more predisposed to *DNA damage* and *lung tumors* than the other groups. Finally, NA inhalation induces acute cytotoxicity in young mice at NA vapor levels that are below the current national exposure limits set by the OSHA and the National Institute for Occupational Safety and Health (10 ppm), which further highlights the special susceptibility of the developing lung to NA exposure-related toxicity.

Table 2. Significantly Changed CYP- and GSH-Related Genes NA Exposed Versus Unexposed at Each Age

Gene	Gene Name	Fold Change Exposed Versus Unexposed at each age					
		Male Neonate	Male Juvenile	Male Adult	Female Neonate	Female Juvenile	Female Adult
Cyp19a1	Cytochrome P450, family 19, subfamily a, polypeptide 1		−3.16	−2.42		−4.55	−2.59
Cyp2f2	Cytochrome P450, family 2, subfamily f, polypeptide 2		−7.32	−4.79		−9.54	−4.95
Gclc	Glutamate-cysteine ligase, catalytic subunit			1.58		1.46	
Gclm	Glutamate-cysteine ligase, modifier subunit						
Gpx1	Glutathione peroxidase 1			−1.33			−1.32
Gpx3	Glutathione peroxidase 3						
Gpx4	Glutathione peroxidase 4			−2.03			−1.77
Gpx5	Glutathione peroxidase 5						
Gpx6	Glutathione peroxidase 6		−2.45	−1.89		−6.5	−2.95
Gpx7	Glutathione peroxidase 7						
Gsr	Glutathione reductase						
Gss	Glutathione synthetase			−1.63			−1.53
Gsta3	Glutathione S-transferase, alpha 3		−2.82	−2.32		−4.07	−1.66
Gsta4	Glutathione S-transferase, alpha 4		−2.31	−2.33		−2.46	−1.88
Gstk1	Glutathione S-transferase kappa 1		−1.87	−2.32		−2.43	−2.02
Gstm2	Glutathione S-transferase, mu 2	1.34		−1.45		−1.65	−1.8
Gstm3	Glutathione S-transferase, mu 3			−1.74		−1.98	
Gstm4	Glutathione S-transferase, mu 4		−1.93	−2.05		−2.3	−1.83
Gstm5	Glutathione S-transferase, mu 5		−1.59	−1.94		−1.42	−1.45
Gsto2	Glutathione S-transferase omega 2						
Gstp1	Glutathione S-transferase, pi 1						
Gstt1	Glutathione S-transferase, theta 1			−2.2			−2.11
Gstt2	Glutathione S-transferase, theta 2	1.29					

SUPPLEMENTARY DATA

Supplementary data are available at *Toxicological Sciences* online.

DECLARATION OF CONFLICTING INTERESTS

The authors declared no potential conflicts of interest with respect to the research, authorship, and publication of this article.

ACKNOWLEDGMENTS

We would like to thank Dr Michele La Merrill as well as all participants in Laura Van Winkle's Air Pollution Journal Club for their valuable feedback on this manuscript. Histologic sectioning was assisted by Jonathan Jennings-Navarro, Kelly Keum, Arianne Medrano, Jeffrey Brown, Chelsea Tasani, and Randall Tran. Imaging for stereology was assisted by Alisha Seabert and Kelly Keum. Microdissection of lung tissues was assisted by Patti Edwards and Alisha Seabert. RNA preparation was completed in part by Chelsea Leigh Tasani. The NanoString gene expression assay processing was carried out by the DNA Technologies and Expression Analysis Cores at the UC Davis Genome Center by Cheryl Tan (Nanostring) and Vanessa Rashbrook (UC Davis Genome Center Core). We are extremely grateful to Cheryl Tan for providing additional assistance with the Nanostring analysis, and to Angela Mendenhall (Nanostring) for providing methods validation support.

FUNDING

During the period this research was conducted, Sarah Carratt was supported by a Robert Emrie Smith Memorial Research Fellowship and a NIEHS T32 Fellowship T32 ES007059. Research was funded by NIEHS Grants R01 ES020867 and R01 ES020867S1. Additional support was provided by UC Davis Cellular and Molecular Imaging Core and UC Davis Environmental Health Sciences Core Center (P30 ES023513). The DNA Technologies and Expression Analysis Core at the UC Davis Genome Center is supported by NIH Shared Instrumentation Grant S10 OD010786.

REFERENCES

Abdo, K., Eustis, S. L., McDonald, M., Jokinen, M. P., Adkins, B., and Haseman, J. K. (1992). Naphthalene: A respiratory tract toxicant and carcinogen for mice. *Inhal. Toxicol.* **4**, 393–409.

Abdo, K. M., Grumbein, S., Chou, B. J., and Herbert, R. (2001). Toxicity and carcinogenicity study in F344 rats following 2 years of whole-body exposure to naphthalene vapors. *Inhal. Toxicol.* **13**, 931–950.

Al-Daghri, N. M. (2008). Serum polycyclic aromatic hydrocarbons among children with and without asthma: Correlation to environmental and dietary factors. *Int. J. Occup. Med. Environ. Health* **21**, 211–217.

An, G., Tesfaigzi, J., Carlson, D. M., and Wu, R. (1993). Expression of a squamous cell marker, the spr1 gene, is posttranscriptionally down-regulated by retinol in airway epithelium. *J. Cell Physiol.* **157**, 562–568.

Buchholz, B. A., Carratt, S. A., Kuhn, E. A., Collette, N. M., Ding, X., and Van Winkle, L. S. (2019). Naphthalene DNA adduct

formation and tolerance in the lung. *Nucl. Instrum. Methods Phys. Res. B* **438**, 119–123.

Buckpitt, A., Boland, B., Isbell, M., Morin, D., Shultz, M., Baldwin, R., Chan, K., Karlsson, A., Lin, C., and Taff, A. (2002). Naphthalene-induced respiratory tract toxicity: Metabolic mechanisms of toxicity. *Drug Metab. Rev.* **34**, 791–820.

Buckpitt, A., Buonarati, M., Avey, L. B., Chang, A. M., Morin, D., and Plopper, C. G. (1992). Relationship of cytochrome P450 activity to Clara cell cytotoxicity. II. Comparison of stereoselectivity of naphthalene epoxidation in lung and nasal mucosa of mouse, hamster, rat and rhesus monkey. *J. Pharmacol. Exp. Ther.* **261**, 364–372.

Buckpitt, A., Chang, A. M., Weir, A., Van Winkle, L., Duan, X., Philpot, R., and Plopper, C. (1995). Relationship of cytochrome P450 activity to Clara cell cytotoxicity. IV. Metabolism of naphthalene and naphthalene oxide in microdissected airways from mice, rats, and hamsters. *Mol. Pharmacol.* **47**, 74–81.

Buckpitt, A., Kephalopoulos, S., Koistinen, K., Kotzias, D., Morawska, L., and Sagunski, H. (2010). Naphthalene. In *WHO Guidelines for Indoor Air Quality: Selected Pollutants*, Geneva.

Buckpitt, A. R., and Warren, D. L. (1983). Evidence for hepatic formation, export and covalent binding of reactive naphthalene metabolites in extrahepatic tissues in vivo. *J. Pharmacol. Exp. Ther.* **225**, 8–16.

Carratt, S. A., Hartog, M., Buchholz, B. A., Kuhn, E. A., Collette, N. M., Ding, X., and Van Winkle, L. S. (2019). Naphthalene genotoxicity: DNA adducts in primate and mouse airway explants. *Toxicol. Lett.* **305**, 103–109.

Chan, J. K., Charrier, J. G., Kodani, S. D., Vogel, C. F., Kado, S. Y., Anderson, D. S., Anastasio, C., and Van Winkle, L. S. (2013). Combustion-derived flame generated ultrafine soot generates reactive oxygen species and activates Nrf2 antioxidants differently in neonatal and adult rat lungs. *Part Fibre Toxicol.* **10**, 34.

Chichester, C. H., Buckpitt, A. R., Chang, A., and Plopper, C. G. (1994). Metabolism and cytotoxicity of naphthalene and its metabolites in isolated murine Clara cells. *Mol. Pharmacol.* **45**, 664–672.

Chichester, C. H., Philpot, R. M., Weir, A. J., Buckpitt, A. R., and Plopper, C. G. (1991). Characterization of the cytochrome P-450 monooxygenase system in nonciliated bronchiolar epithelial (Clara) cells isolated from mouse lung. *Am. J. Respir. Cell Mol. Biol.* **4**, 179–186.

Cho, T. M., Rose, R. L., and Hodgson, E. (2005). In vitro metabolism of naphthalene by human liver microsomal cytochrome P450 enzymes. *Drug Metab. Dispos.* **34**, 176. 10.1124/dmd.105.005785).

Chuang, J. C., Callahan, P. J., Lyu, C. W., and Wilson, N. K. (1999). Polycyclic aromatic hydrocarbon exposures of children in low-income families. *J. Expo Anal. Environ. Epidemiol.* **9**, 85–98.

Cruzan, G., Bus, J., Banton, M., Gingell, R., and Carlson, G. (2009). Mouse specific lung tumors from CYP2F2-mediated cytotoxic metabolism: An endpoint/toxic response where data from multiple chemicals converge to support a mode of action. *Regul. Toxicol. Pharmacol.* **55**, 205–218.

Devereux, T. R., Domin, B. A., and Philpot, R. M. (1989). Xenobiotic metabolism by isolated pulmonary cells. *Pharmacol. Ther.* **41**, 243–256.

Duan, X., Plopper, C., Brennan, P., and Buckpitt, A. (1996). Rates of glutathione synthesis in lung subcompartments of mice and monkeys: Possible role in species and site selective injury. *J. Pharmacol. Exp. Ther.* **277**, 1402–1409.

Evans, M. J., Van Winkle, L. S., Fanucchi, M. V., and Plopper, C. G. (1999). The attenuated fibroblast sheath of the respiratory tract epithelial- mesenchymal trophic unit. *Am. J. Respir. Cell Mol. Biol.* **21**, 655–657.

Fanucchi, M. V., Buckpitt, A. R., Murphy, M. E., and Plopper, C. G. (1997). Naphthalene cytotoxicity of differentiating Clara cells in neonatal mice. *Toxicol. Appl. Pharmacol.* **144**, 96–104.

Fanucchi, M. V., Buckpitt, A. R., Murphy, M. E., Storms, D. H., Hammock, B. D., and Plopper, C. G. (2000). Development of phase II xenobiotic metabolizing enzymes in differentiating murine Clara cells. *Toxicol. Appl. Pharmacol.* **168**, 253–267.

Fanucchi, M. V., Murphy, M. E., Buckpitt, A. R., Philpot, R. M., and Plopper, C. G. (1997). Pulmonary cytochrome P450 monooxygenase and Clara cell differentiation in mice. *Am. J. Respir. Cell Mol. Biol.* **17**, 302–314.

Hawthorn, L., Stein, L., Panzarella, J., Loewen, G. M., and Baumann, H. (2006). Characterization of cell-type specific profiles in tissues and isolated cells from squamous cell carcinomas of the lung. *Lung Cancer* **53**, 129–142.

Howard, V., and Reed, M. G. (1998). *Unbiased Stereology: Three-Dimensional Measurement in Microscopy*. Springer, New York.

Hsia, C. C., Hyde, D. M., Ochs, M., Weibel, E. R.; ATS/ERS Joint Task Force on Quantitative Assessment of Lung. (2010). An official research policy statement of the American Thoracic Society/European Respiratory Society: Standards for quantitative assessment of lung structure. *Am. J. Respir. Crit. Care Med.* **181**, 394–418.

Kanekal, S., Plopper, C., Morin, D., and Buckpitt, A. (1991). Metabolism and cytotoxicity of naphthalene oxide in the isolated perfused mouse lung. *J. Pharmacol. Exp. Ther.* **256**, 391–401.

Kovalchuk, N., Kelty, J., Li, L., Hartog, M., Zhang, Q. Y., Edwards, P., Van Winkle, L., and Ding, X. (2017). Impact of hepatic P450-mediated biotransformation on the disposition and respiratory tract toxicity of inhaled naphthalene. *Toxicol. Appl. Pharmacol.* **329**, 1–8.

Kramer, A., Green, J., Pollard, J., Jr, and Tugendreich, S. (2014). Causal analysis approaches in ingenuity pathway analysis. *Bioinformatics* **30**, 523–530.

Li, L., Carratt, S., Hartog, M., Kovalchuk, N., Jia, K., Wang, Y., Zhang, Q.-Y., Edwards, P., Winkle, L. V., and Ding, X. (2017). Human CYP2A13 and CYP2F1 mediate naphthalene toxicity in the lung and nasal mucosa of CYP2A13/2F1-humanized mice. *Environ. Health Perspect.* **125**, 067004.

Li, L., Wei, Y., Van Winkle, L., Zhang, Q. Y., Zhou, X., Hu, J., Xie, F., Kluetzman, K., and Ding, X. (2011). Generation and characterization of a Cyp2f2-null mouse and studies on the role of CYP2F2 in naphthalene-induced toxicity in the lung and nasal olfactory mucosa. *J. Pharmacol. Exp. Ther.* **339**, 62–71.

Li, Z., Sandau, C. D., Romanoff, L. C., Caudill, S. P., Sjodin, A., Needham, L. L., and Patterson, D. G., Jr. (2008). Concentration and profile of 22 urinary polycyclic aromatic hydrocarbon metabolites in the US population. *Environ. Res.* **107**, 320–331.

Lin, R. L., Sargeant, S., and Narasimhachari, N. (1974). Indolethylamine-N-methyltransferase in developing rabbit lung. *Dev. Psychobiol.* **7**, 475–481.

National Toxicology Program (1992). Toxicology and carcinogenesis studies of naphthalene (CAS No. 91-20-3) in B6C3F1 mice (inhalation studies). *Natl. Toxicol. Prog. Tech. Rep. Ser.* **410**, 1–172.

National Toxicology Program (2000). Toxicology and carcinogenesis studies of naphthalene (cas no. 91-20-3) in F344/N rats (inhalation studies). *Natl. Toxicol. Prog. Tech. Rep. Ser.*, 1–173.

Navab, R., Strumpf, D., Bandarchi, B., Zhu, C. Q., Pintilie, M., Ramnarine, V. R., Ibrahimov, E., Radulovich, N., Leung, L., Barczyk, M., *et al.* (2011). Prognostic gene-expression signature of carcinoma-associated fibroblasts in non-small cell lung cancer. *Proc. Natl. Acad. Sci. U.S.A.* **108**, 7160–7165.

Orjuela, M. A., Liu, X., Miller, R. L., Warburton, D., Tang, D., Jobanputra, V., Hoepner, L., Suen, I. H., Diaz-Carreno, S., Li, Z., *et al.* (2012). Urinary naphthol metabolites and chromosomal aberrations in 5-year-old children. *Cancer Epidemiol. Biomark. Prev.* **21**, 1191–1202.

Phimister, A. J., Lee, M. G., Morin, D., Buckpitt, A. R., and Plopper, C. G. (2004). Glutathione depletion is a major determinant of inhaled naphthalene respiratory toxicity and naphthalene metabolism in mice. *Toxicol. Sci.* **82**, 268–278.

Phimister, A. J., Williams, K. J., Van Winkle, L. S., and Plopper, C. G. (2005). Consequences of abrupt glutathione depletion in murine Clara cells: Ultrastructural and biochemical investigations into the role of glutathione loss in naphthalene cytotoxicity. *J. Pharmacol. Exp. Ther.* **314**, 506–513.

Plopper, C. G., Chang, A. M., Pang, A., and Buckpit, A. R. (1991). Use of microdissected airways to define metabolism and cytotoxicity in murine bronchiolar epithelium. *Exp. Lung Res.* **17**, 197–212.

Plopper, C. G., Cranz, D. L., Kemp, L., Serabjit-Singh, C. J., and Philpot, R. M. (1987). Immunohistochemical demonstration of cytochrome P-450 monooxygenase in Clara cells throughout the tracheobronchial airways of the rabbit. *Exp. Lung Res.* **13**, 59–68.

Plopper, C. G., and Hyde, D. M. (1992a). Epithelial cells of bronchioles. In *Comparative Biology of the Normal Lung (R.A. Parent, Ed.)*, Vol. **1**, pp. 85-92. CRC Press, Boca Raton.

Plopper, C. G., Macklin, J., Nishio, S. J., Hyde, D. M., and Buckpitt, A. R. (1992b). Relationship of cytochrome P-450 activity to Clara cell cytotoxicity. III. Morphometric comparison of changes in the epithelial populations of terminal bronchioles and lobar bronchi in mice, hamsters, and rats after parenteral administration of naphthalene. *Lab. Invest.* **67**, 553–565.

Plopper, C. G., Suverkropp, C., Morin, D., Nishio, S., and Buckpitt, A. (1992c). Relationship of cytochrome P-450 activity to Clara cell cytotoxicity. I. Histopathologic comparison of the respiratory tract of mice, rats and hamsters after parenteral administration of naphthalene. *J. Pharmacol. Exp. Ther.* **261**, 353–363.

Plopper, C. G., Van Winkle, L. S., Fanucchi, M. V., Malburg, S. R., Nishio, S. J., Chang, A., and Buckpitt, A. R. (2001). Early events in naphthalene-induced acute Clara cell toxicity. II. Comparison of glutathione depletion and histopathology by airway location. *Am. J. Respir. Cell Mol. Biol.* **24**, 272–281.

Sengupta, S., and Harris, C. C. (2005). p53: Traffic cop at the crossroads of DNA repair and recombination. *Nat. Rev. Mol. Cell Biol.* **6**, 44–55.

Shen, L., Yang, M., Lin, Q., Zhang, Z., Zhu, B., and Miao, C. (2016). COL11A1 is overexpressed in recurrent non-small cell lung cancer and promotes cell proliferation, migration, invasion and drug resistance. *Oncol. Rep.* **36**, 877–885.

Sutherland, K. M., Combs, T. J., Edwards, P. C., and Van Winkle, L. S. (2010). Site-specific differences in gene expression of secreted proteins in the mouse lung: Comparison of methods to show differences by location. *J. Histochem. Cytochem.* **58**, 1107–1119.

Tesfaigzi, J., Th'ng, J., Hotchkiss, J. A., Harkema, J. R., and Wright, P. S. (1996). A small proline-rich protein, SPRR1, is upregulated early during tobacco smoke-induced squamous metaplasia in rat nasal epithelia. *Am. J. Respir. Cell Mol. Biol.* **14**, 478–486.

USEPA (1998). Toxicological Review of Naphthalene, 1–42.

Van Winkle, L. S., Buckpitt, A. R., Nishio, S. J., Isaac, J. M., and Plopper, C. G. (1995). Cellular response in naphthalene-induced Clara cell injury and bronchiolar epithelial repair in mice. *Am. J. Physiol.* **269**, L800–L818.

Van Winkle, L. S., Buckpitt, A. R., and Plopper, C. G. (1996). Maintenance of differentiated murine Clara cells in microdissected airway cultures. *Am. J. Respir. Cell Mol. Biol.* **14**, 586–598.

Van Winkle, L. S., Evans, M. J., Brown, C. D., Willits, N. H., Pinkerton, K. E., and Plopper, C. G. (2001). Prior exposure to aged and diluted sidestream cigarette smoke impairs bronchiolar injury and repair. *Toxicol. Sci.* **60**, 152–164.

Wang, K. K., Liu, N., Radulovich, N., Wigle, D. A., Johnston, M. R., Shepherd, F. A., Minden, M. D., and Tsao, M. S. (2002). Novel candidate tumor marker genes for lung adenocarcinoma. *Oncogene* **21**, 7598–7604.

Warren, D. L., Brown, D., Jr., and Buckpitt, A. R. (1982). Evidence for cytochrome P-450 mediated metabolism in the bronchiolar damage by naphthalene. *Chem. Biol. Interact.* **40**, 287–303.

West, J. A., Buckpitt, A. R., and Plopper, C. G. (2000). Elevated airway GSH resynthesis confers protection to Clara cells from naphthalene injury in mice made tolerant by repeated exposures. *J. Pharmacol. Exp. Ther.* **294**, 516–523.

West, J. A., Pakehham, G., Morin, D., Fleschner, C. A., Buckpitt, A. R., and Plopper, C. G. (2001). Inhaled naphthalene causes dose dependent Clara cell cytotoxicity in mice but not in rats. *Toxicol. Appl. Pharmacol.* **173**, 114–119.